An EPR study of rareearth impurities in single crystals of the zircon structure orthophosphates ScPO4, YPO4, and LuPO4a)

M. M. Abraham, L. A. Boatner, J. O. Ramey, and M. Rappaz

Citation: J. Chem. Phys. **78**, 3 (1983); doi: 10.1063/1.444516
View online: http://dx.doi.org/10.1063/1.444516
View Table of Contents: http://jcp.aip.org/resource/1/JCPSA6/v78/i1
Published by the American Institute of Physics.

An EPR study of rare-earth impurities in single crystals of the zircon-structure orthophosphates $ScPO_4$, YPO_4, and $LuPO_4$[a)]

M. M. Abraham, L. A. Boatner, J. O. Ramey, and M. Rappaz[b)]

Solid State Division, Oak Ridge National Laboratory, Oak Ridge, Tennessee 37830
(Received 4 August 1982; accepted 13 September 1982)

Ceramic materials based on the lanthanide orthophosphate series of compounds are known to be highly stable both chemically and physically. These characteristics have recently led to an extensive evaluation of these substances as potential primary containment media for the disposal of high-level radioactive wastes. Since one important class of high-level nuclear waste (i.e., reprocessed light water reactor spent fuel) contains a relatively high concentration of various lanthanides, the solid state chemical properties of the mixed rare-earth and actinide-doped orthophosphates are of considerable practical interest. The Kramers' ions Ce^{3+}, Nd^{3+}, Dy^{3+}, Er^{3+}, Yb^{3+}, and U^{3+} have been incorporated in single crystals of the tetragonal symmetry hosts $ScPO_4$, YPO_4, and $LuPO_4$, and EPR spectroscopy has been used to verify the substitutional behavior of these ions and to investigate their electronic ground state properties. Principal axial spectroscopic splitting factors and hyperfine parameters were determined. These results are compared to those obtained for the same paramagnetic ions in other hosts characterized by crystal fields with tetragonal symmetry at the impurity-ion site.

I. INTRODUCTION

At elevated temperatures, the lanthanide orthophosphates ($LnPO_4$ with Ln = La, Ce, Pr, ..., Lu) crystallize into two different structural types. Orthophosphates of the first half of the lanthanide transition series crystallize in a monoclinic form, while orthophosphates of the second half of the series, as well as YPO_4 and $ScPO_4$, crystallize with a tetragonal structure. The monoclinic lanthanide orthophosphate form is a direct structural analog of the natural mixed rare-earth mineral monazite,[1] while the tetragonal form is the structural analog of the minerals, zircon ($ZrSiO_4$) and xenotime (YPO_4). Both rare-earth orthophosphate structural types exhibit characteristics that make them attractive as potential high-level radioactive waste forms.[2–4] These characteristics include an established long-term stability ($\sim 2\times10^9$ y) in various geological situations, a known ability to incorporate relatively high concentrations of the actinides, thorium, and uranium, and an apparently high degree of resistance to permanent metamictization due to α particle and nuclear recoil damage. The potentially important application of lanthanide orthophosphates as a primary nuclear waste form has provided the motivation for a series of studies of the physical and chemical characteristics of mixed orthophosphate-impurity systems. In particular, electron paramagnetic resonance (EPR) spectroscopy has been applied to the determination of site symmetries and valence states for a number of impurities in both single crystal and polycrystalline samples of this class of materials.[5–8] Additional investigations of the properties of both pure and doped rare-earth phosphates have been carried out using optical absorption,[9–11] x-ray diffraction,[12] and Raman spectroscopy.[13]

The results of the previous studies show that, in the monoclinic monazite unit cell, there are four different lanthanide sites that can be effectively reduced to two different pairs of magnetic sites as a result of inversion symmetry. The local crystalline-electric field is identical at the four lanthanide positions. Therefore, in a magnetic resonance experiment, two generally magnetically inequivalent spectra are observed at arbitrary applied magnetic-field orientations, and each spectrum arises from two magnetically equivalent sites in the structure. In the case of the tetragonal zircon-structure orthophosphates, all of the lanthanide sites are generally magnetically equivalent, and thus, only one EPR spectrum is observed at any given magnetic-field orientation. This reduced complexity greatly simplifies the interpretation of the EPR spectra of impurities in the tetragonal symmetry hosts. As part of the continuing study of orthophosphate properties, the present work reports the results of EPR investigations of the dopant ions Ce^{3+}, Nd^{3+}, Dy^{3+}, Er^{3+}, Yb^{3+}, and U^{3+} in the tetragonal orthophosphate single crystals $ScPO_4$, YPO_4, and $LuPO_4$.

II. EXPERIMENTAL

Doped single crystals of $ScPO_4$, YPO_4, and $LuPO_4$ were grown[14] by first reacting the appropriate host and dopant oxides with lead hydrogen phosphate in a platinum crucible at 1360 °C and then slowly cooling the resulting mixture of $Pb_2P_2O_7$ plus orthophosphate at a rate of ~ 1 °C h^{-1} between 1360 and 900 °C. After cooling to room temperature from 900 °C, the resulting single crystals are freed from the solidified lead pyrophosphate by dissolving the flux with boiling nitric acid.

Two different EPR superheterodyne spectrometers operating at 3 cm (X band) and 1.2 cm (K band) were employed in the resonance studies. A maximum magnetic field of 12 kG was available. The applied magnetic field values were determined by means of a proton mag-

[a)] Research sponsored by the Division of Materials Sciences, U.S. Department of Energy under contract W-7405-Eng-26 with the Union Carbide Corporation.

[b)] Present address: Ecole Polytechnique Fédérale de Lausanne, Département des Materiaux, CH-1007 Lausanne, Switzerland.

 0021-9606/83/010003-08$02.10

netic resonance probe, and both the proton resonance and the microwave frequencies were measured using a Hewlett Packard HP-5245L frequency counter with an HP-5255A frequency converter. All of the measurements were performed on samples that were cooled to a temperature of 4.2 K or below. A special sample holder was used to rotate the crystals in a vertical plane inside the microwave cavity, and this rotation, combined with the external horizontal rotation of the magnetic field, was used to obtain an accurate alignment of the principal axes of the sample with the magnetic field. The presence of additional unwanted paramagnetic impurities, coupled with the large anisotropy of the resonance signals as a function of the crystal orientation, often resulted in complex mixed EPR spectra. Difficulties of this type were frequently circumvented by doping the host crystals with isotopically enriched impurities.

III. RESULTS AND DISCUSSION

For each of the dopants investigated here, determinations of the principal ground state g values and hyperfine parameters were made. The principal g values have been used in identifying the dominant character of the ground state wave functions where appropriate. In the following sections, results are presented for each dopant beginning with cerium, continuing in order of increasing number of $4f$ electrons, and finally ending with the $5f^3$ configuration ion U^{3+}. The results were interpreted using the usual spin-Hamiltonian of the following form:

$$\mathcal{H} = g_{\parallel}\mu_B H_z S_z + g_{\perp}\mu_B [H_x S_x + H_y S_y] + A_{\parallel} I_z S_z + A_{\perp}[I_x S_x + I_y S_y] , \quad (1)$$

where μ_B is the Bohr magneton, H is the applied magnetic field, and an effective spin of $S = 1/2$ is employed. The parallel and perpendicular components of the g and A tensors lie along the crystallographic c and a axes, respectively, and the relationship between these axes and the $Ln{-}O_8$ complex has been given previously in Ref. 12.

A. Trivalent cerium

Ce^{3+} has a $4f^1$ electronic configuration and a $^2F_{5/2}$ free-ion ground state. In $ScPO_4$, YPO_4, and $LuPO_4$, the sixfold degeneracy of the ground state is split by the tetragonal crystal field into three Kramers' doublets and the EPR spectrum observed at 4.2 K results from a transition within the lowest lying doublet. The fourfold nature of the crystal field will result in admixtures of states whose M_J values differ by ± 4, and hence, the ground doublet will have a wave function which will be either a pure $|\pm 1/2\rangle$ state or an admixed $\alpha|\pm 5/2\rangle + \beta|\mp 3/2\rangle$ state. The former wave function would yield g values of λ and 3λ for $g_{\parallel}$ and $g_{\perp}$, respectively, while for the latter wave function the g values would be $g_{\parallel} = \lambda[5\alpha^2 - 3\beta^2]$ and $g_{\perp} = (\sqrt{20})\ \alpha\beta\lambda$. [Here λ is the Landé g factor which for Ce^{3+} would be equal to 6/7 to first order.] The EPR spectrum of Ce^{3+}, which consists of a single resonance line, was observed in all three hosts and the measured principal g values are listed in Table I. The spectral line width increased as the applied magnetic field was rotated from a direction perpendicular to the crystal c axis to a direction parallel to the axis. Due to the significantly increased line width near the parallel orientation, the parallel g value was determined in all three hosts by means of a least-squares fit of the resonance magnetic field value plotted vs $\cos^2\theta$. An identification of the ground doublet as being the pure $|\pm\frac{1}{2}\rangle$ wave function is precluded by the fact that $g_{\perp} \neq 3\ g_{\parallel}$. Using the experimentally determined g values, values of α and β may be obtained for the wave function $\alpha|\pm 5/2\rangle + \beta|\mp 3/2\rangle$ which yield consistent and reasonable values for the Landé g factor λ. These λ values are, however, all less than the first order value of 6/7. This reduction in the Landé g factor is not unexpected and can probably be attributed to appreciable admixtures of excited states into the Ce^{3+} ground state.[15]

TABLE I. Ground state g values for rare-earth impurities in the tetragonal-symmetry hosts $ScPO_4$, YPO_4, and $LuPO_4$.[a]

	$ScPO_4$	YPO_4	$LuPO_4$
Ce^{3+}	$g_{\parallel} = 0.44(2)$	$g_{\parallel} = 0.63(2)$	$g_{\parallel} = 0.2(2)$
	$g_{\perp} = 1.476(1)$	$g_{\perp} = 1.713(1)$	$g_{\perp} = 1.656(1)$
	$\bar{g} = 1.131$	$\bar{g} = 1.352$	$\bar{g} = 1.171$
Nd^{3+}	$g_{\parallel} = 2.199(1)$	$g_{\parallel} = 3.092(2)$	$g_{\parallel} = 2.842(2)$
	$g_{\perp} = 1.592(1)$	$g_{\perp} = 1.224(1)$	$g_{\perp} = 1.339(1)$
	$\bar{g} = 1.794$	$\bar{g} = 1.847$	$\bar{g} = 1.840$
Er^{3+}	$g_{\parallel} = 5.784(6)$	$g_{\parallel} = 6.438(6)$	$g_{\parallel} = 6.345(6)$
	$g_{\perp} = 5.490(6)$	$g_{\perp} = 4.803(6)$	$g_{\perp} = 4.968(6)$
	$\bar{g} = 5.588$	$\bar{g} = 5.348$	$\bar{g} = 5.427$
Yb^{3+}	$g_{\parallel} = 0.973(2)$	$g_{\parallel} = 1.526(1)$	$g_{\parallel} = 1.338(10)$
	$g_{\perp} = 3.405(3)$	$g_{\perp} = 3.120(3)$	$g_{\perp} = 3.233(3)$
	$\bar{g} = 2.594$	$\bar{g} = 2.589$	$\bar{g} = 2.601$
U^{3+}	$g_{\parallel} = 1.370(1)$	...	$g_{\parallel} = 3.13(1)$
	$g_{\perp} = 1.736(1)$	...	$g_{\perp} = 0.9(1)$
	$\bar{g} = 1.614$	...	$\bar{g} = 1.643$
Dy^{3+}	...	...	$g_{\parallel} = 11.26(5)$
	...	...	$g_{\perp} \approx 4.2$
	...	...	$\bar{g} \approx 6.6$

[a]Only absolute values are given.

Trivalent cerium has previously been observed in tetragonal symmetry sites in the alkaline earth fluorides CaF_2, SrF_2, and BaF_2[16–20] and in the scheelite-structure hosts $CaWO_4$, $SrWO_4$, $BaMoO_4$, and $PbMoO_4$.[21–23] In these hosts $g_{\parallel}$ varied from 2.6 to 3.0 and $g_{\perp}$ varied in the range of 1.4 to 1.6. In all of these cases the mean value, $\bar{g} = (g_{\parallel} + 2g_{\perp})/3$, is close to the maximum mean value of $2\lambda(J+1)/3 = 2$ as discussed by Rubins.[24] For the case of Ce^{3+} in the three orthophosphates studied here, however, $g_{\perp}$ is greater than $g_{\parallel}$ and the mean $\bar{g}$ value (see Table I) is lower and closer to the other value $2\lambda J/3 = 1.4$ mentioned by Rubins.[24] Nevertheless, the form of the wave function is not different in the present and previously noted cases. A second tetragonal cerium spectrum in CaF_2 doped with Na has been reported by McLaughlan[19] which also has $g_{\perp}$ ($= 2.402$) $> g_{\parallel}$ ($= 0.725$) but in that case the mean $\bar{g}$ value is larger than in the orthophosphates and is closer to the maximum value noted above.

B. Trivalent neodymium

Nd^{3+} has the $4f^3$ electronic configuration and a $^4I_{9/2}$ free-ion ground state. The tenfold degeneracy of the ground state is split by the tetragonal crystal field into five Kramers' doublets, and the ground doublet will have a wave function either of the form of

$$a|\pm 9/2\rangle + b|\pm 1/2\rangle + c|\mp 7/2\rangle$$

or of

$$a|\pm 5/2\rangle + b|\mp 3/2\rangle \ .$$

EPR spectra due to Nd^{3+} in tetragonal-symmetry substitutional sites were detected in all three orthophosphate hosts at $T = 4.2$ K. Figure 1 shows the spectra obtained from a YPO_4 crystal doped with isotopically enriched Nd-143 and Fig. 2 shows the corresponding spectra obtained using enriched Nd-145. Additional lines, due to Er^{3+} and Gd^{3+} impurities, are also present. The Gd^{3+} fine structure has been previously measured and identified in these same hosts using the higher microwave frequency of 35 GHz.[7] These previous identifications were helpful in separating the Gd^{3+} fine structure from the Nd^{3+} spectrum at the lower microwave frequency of 9 GHz. Moreover, since the positions of the Gd^{3+} resonance transitions are extremely sensitive to the crystal orientation relative to the magnetic field, these transitions were useful both as an aid in achieving the crystal orientation and for verifications of the final crystal position.

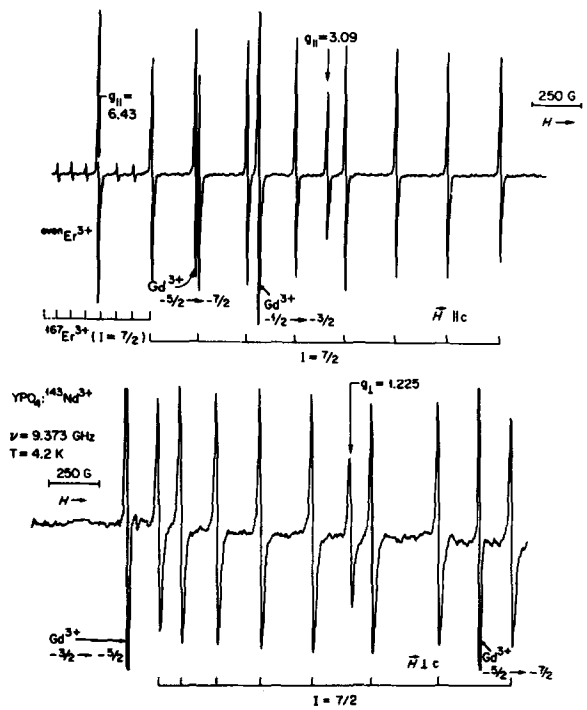

FIG. 1. EPR spectra of a YPO_4 crystal doped with isotopically enriched neodymium-143. Top trace—spectrum with H parallel to the c axis of the crystal; bottom trace—spectrum with H perpendicular to the c axis of the crystal. Neodymium-143 hyperfine lines are indicated by the bar diagrams below the spectra. Extra lines due to unintentional impurities of erbium and gadolinium are also present. The transitions due to Gd^{3+} are labeled by their appropriate M_s designations according to the known negative sign for b_2^0 in this host [Ref. 7]. The extra lines serve to verify the crystal orientation.

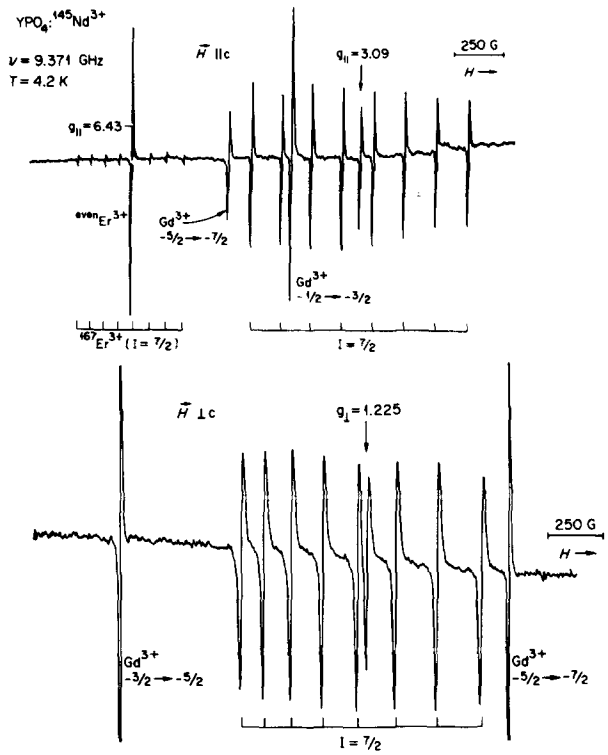

FIG. 2. EPR spectra of a YPO_4 crystal doped with isotopically enriched neodymium-145. Top trace—spectrum with H parallel to the c axis of the crystal; bottom trace—spectrum with H perpendicular to the c axis. Neodymium-145 hyperfine lines are indicated by the bar diagrams below the traces. Additional lines due to gadolinium and erbium impurities are also identified and bar diagrams identify the erbium-167 (~ 23% natural abundance) hyperfine lines and the different gadolinium fine structure lines.

The experimental g values and hyperfine parameters obtained for Nd^{3+} are listed in Tables I and II, respec-

TABLE II. Hyperfine parameters (in MHz) for rare-earth impurities in the tetragonal-symmetry hosts $ScPO_4$, YPO_4, and $LuPO_4$.[a]

	$ScPO_4$	YPO_4	$LuPO_4$
^{143}Nd	$A_{\parallel} = 790(1)$	$A_{\parallel} = 1054(2)$	$A_{\parallel} = 981(2)$
	$A_{\perp} = 542(1)$	$A_{\perp} = 425(1)$	$A_{\perp} = 462(1)$
^{145}Nd	$A_{\parallel} = 491(1)$	$A_{\parallel} = 657(1)$	$A_{\parallel} = 611(1)$
	$A_{\perp} = 336(1)$	$A_{\perp} = 261(1)$	$A_{\perp} = 285(1)$
^{167}Er	$A_{\parallel} = 603(2)$	$A_{\parallel} = 669(2)$	$A_{\parallel} = 662(2)$
	$A_{\perp} = 575(2)$	$A_{\perp} = 503(2)$	$A_{\perp} = 520(2)$
^{171}Yb	$A_{\parallel} = 786(8)$	$A_{\parallel} = 1223(12)$	$A_{\parallel} = 1081(10)$
	$A_{\perp} = 2692(20)$	$A_{\perp} = 2472(20)$	$A_{\perp} = 2558(20)$
^{173}Yb	$A_{\parallel} = 211(1)$	$A_{\parallel} = 332(1)$	$A_{\parallel} = 292(1)$
	$A_{\perp} = 770(2)$	$A_{\perp} = 704(2)$	$A_{\perp} = 730(2)$
^{161}Dy	...	...	$A_{\parallel} = 938(9)$
	...	...	...
^{163}Dy	...	...	$A_{\parallel} = 1324(5)$
	...	...	...

[a]Only absolute values are given.

tively. Elliott and Stevens[25] have shown that when the quantity $g_{\parallel}B/g_{\perp}A$ is close to unity, the admixture of excited states from other J manifolds can be neglected. The experimental results obtained here yield values of 0.95, 1.02, and 1.00 for this quantity for Nd-143 in $ScPO_4$, YPO_4, and $LuPO_4$, respectively. (The corresponding values for Nd-145 are 0.95, 1.00, and 0.99.)

Tetragonal Nd^{3+} spectra have been observed in the cubic fluorides CaF_2[21,26] and SrF_2[26] ($g_{\parallel} > g_{\perp}$) and in crystals of the scheelite series,[22,27,28] ($g_{\parallel} < g_{\perp}$). In both types of host crystals, the mean $\bar{g}$ value ranges from 2 to 2.4. McLaughlan[19] observed a second tetragonal Nd^{3+} spectrum $g_{\parallel} < g_{\perp}$ in CaF_2 which had been doped with Na, but the mean $\bar{g}$ value was in the same 2 to 2.4 range. The mean $\bar{g}$ values for Nd^{3+} in $ScPO_4$, YPO_4, and $LuPO_4$ as listed in Table I are 1.79, 1.85, and 1.84, respectively, and are similar to the value of 1.87 obtained by Ranon[29] for Nd^{3+} in the isostructural host YVO_4. It is believed that the g values for Nd^{3+} in YPO_4 that were reported by Hillmer[30] [i.e., $g_{\parallel} = 1.222(3)$ and $g_{\perp} = 3.080(3)$] were inadvertently interchanged (i.e., that $g_{\parallel}$ was identified by Hillmer as $g_{\perp}$) and that our values are thus in agreement with Hillmer within experimental error.

C. Trivalent dysprosium

Dy^{3+} has a $4f^9$ electronic configuration and a $^6H_{15/2}$ free-ion ground state. The 16-fold degeneracy of the ground state is split by the tetragonal crystal field into eight Kramers' doublets and the wave functions associated with these doublets are either

$$a_1|\pm 15/2\rangle + b_1|\pm 7/2\rangle + c_1|\mp 1/2\rangle + d_1|\mp 9/2\rangle$$

or

$$a_2|\pm 13/2\rangle + b_2|\pm 5/2\rangle + c_2|\mp 3/2\rangle + d_2|\mp 11/2\rangle \ .$$

In this case there are too many parameters to determine the correct form of the ground doublet wave function using EPR data alone. The EPR spectrum of Dy^{3+} was observed in $LuPO_4$ and a value of $g_{\parallel} = 11.26(5)$ was determined. The hyperfine parameters for the odd isotopes 161 and 163 were determined to be: $^{161}A = 938(9)$ and $^{163}A = 1324(5)$ MHz. The spectrum of isotopically enriched Dy-163 in $LuPO_4$ is shown in Fig. 3 with H applied parallel to the fourfold crystal c axis. The spectral parameters were not measured accurately with H perpendicular to the c axis but the $g_{\perp}$ value is in the region of 4.2. The Dy^{3+} spectrum was not observed in $ScPO_4$ or YPO_4.

The g values for the Dy^{3+} ground doublet must lie between zero and $2\lambda J = 15\ (4/3) = 20$ and hence the anisotropy can be quite large. Following Rubins,[24] the maximum mean $\bar{g}$ value would be $\bar{g} = 2\lambda(J+1)/3 = 7.56$. Previous observations of Dy^{3+} EPR spectra in tetragonal symmetry have yielded $\bar{g}$ values of 6.167 and 6.517 in the scheelites $CaWO_4$[31] and $LiYF_4$,[28] respectively, and 7.027, 6.970, and 6.67 for the zircon-type hosts $ZiSiO_4$,[32] YVO_4,[29] and YPO_4,[33] respectively. In $YAsO_4$: Dy^{3+}, $\bar{g}$ values of 7.015 and 6.817 have been measured for the lowest Kramers' doublet and for the first excited Kramers' doublet, respectively.[34] Therefore, our mean $\bar{g}$ value (using $g_{\perp} \sim 4.2$) for the ground doublet Dy^{3+} in $LuPO_4$ of approximately 6.55 appears to be consistent with the previous spectroscopic results.

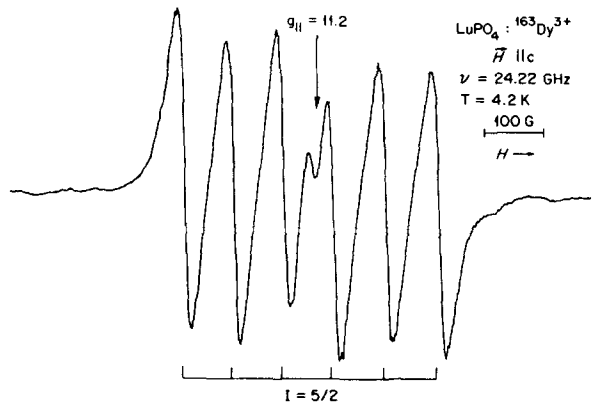

FIG. 3. EPR spectrum of a $LuPO_4$ crystal doped with isotopically enriched dysprosium-163. The magnetic field is parallel to the tetragonal c axis of the crystal. The K-band frequency (24.22 GHz) was employed in preference to an X-band frequency due to the large g value. The small central line arises from residual even–even dysprosium isotopes which have zero nuclear spin and the six large hyperfine lines are due to the isotope ^{163}Dy with a nuclear spin equal to 5/2. The relative intensities are a result of the artificial enrichment.

D. Trivalent erbium

Er^{3+} has a $4f^{11}$ electronic configuration and a $^4I_{15/2}$ free-ion ground state. The tetragonal crystal field splits the 16-fold degeneracy to produce eight Kramers' doublets and the corresponding wave functions have the same general form as those given previously for the case of Dy^{3+}. The Landé factor for the case of Er^{3+} is $\lambda = 6/5$ and the maximum mean $\bar{g}$ value is $\bar{g} = 2\lambda(J+1)/3 = 6.8$. EPR spectra due to Er^{3+} in substitutional sites with tetragonal symmetry were observed in all three orthophosphate hosts at 4.2 K. The EPR spectrum of Er^{3+} with the natural isotopic abundance in the YPO_4 host is shown in Fig. 4 for the parallel and perpendicular directions relative to the c axis. (In Fig. 4, the extra lines due to Gd^{3+} are labeled with their proper M_s designations in accordance with the known negative sign of b_2^0 in this host.[7]) The spectra of isotopically enriched Er-167 impurities incorporated in a $LuPO_4$ single crystal are shown in Fig. 5. The spin-Hamiltonian parameters obtained for Er^{3+} in the three hosts are listed in Tables I and II.

Previous EPR observations of Er^{3+} in sites of tetragonal symmetry have been made for the cubic fluoride hosts CaF_2,[16,35–38] SrF_2[39] and BaF_2,[40] as well as cubic CaO,[41] cubic SrO,[41] and cubic $KMgF_3$.[42] The mean $\bar{g}$ values in these materials range from 6.4 to 6.8. Measurements of tetragonal Er^{3+} spectra in the scheelite series of crystals[28,43–46] have yielded lower $\bar{g}$ values lying in the range 5.8 to 6.4. Included in these results are additional measurements of excited doublets in several crystals.[16,46,47,49,50] The mean $\bar{g}$ values for tetragonal Er^{3+} spectra observed in the zircon structure hosts $YAsO_4$,[51] YPO_4,[52] YVO_4,[29] $ScVO_4$,[53] $ZrSiO_4$,[32,54]

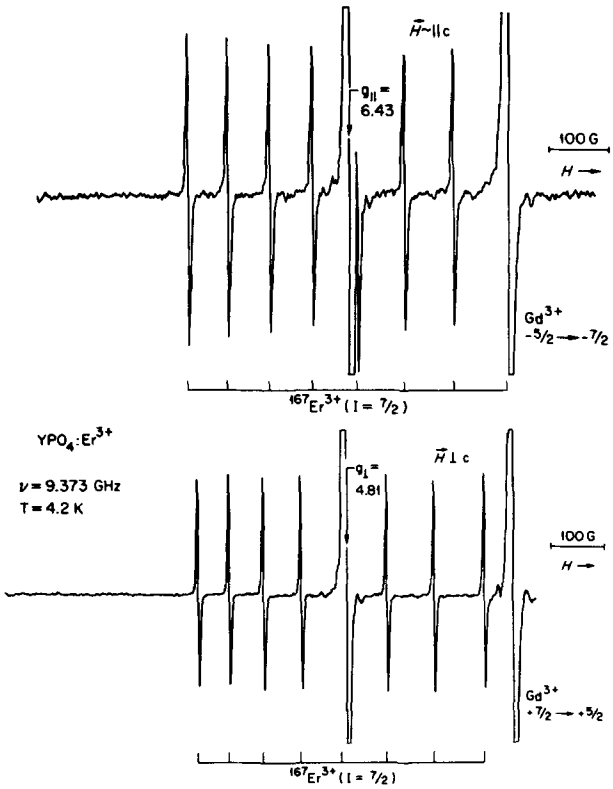

FIG. 4. EPR spectra of a YPO_4 crystal doped with erbium. Top trace—spectrum with H parallel to the c axis of crystal; bottom trace—spectrum with H perpendicular to the c axis. The eight-line hyperfine structure arising from the ~23% naturally abundant isotope, erbium-167, is labeled by the bar diagrams below the traces. The large central lines are due to the even–even isotopes of erbium with zero nuclear spin. Two fine structure lines of Gd^{3+} can also be seen. In the parallel orientation, the highest field erbium-167 hyperfine line is superimposed on a Gd^{3+} transition.

$HfSiO_4$,[54] and $ThSiO_4$[54] are all less than 6 and range from 5.14 in $ScVO_4$[53] to 5.9 in YVO_4.[29] From the data given in Table I, it can be seen that the mean $\bar{g}$ values for the hosts $ScPO_4$, YPO_4, and $LuPO_4$ investigated here, also fall in the middle of this range. Again, in accordance with the work of Elliott and Stevens,[25] the values of $g_\parallel B/g_\perp A$ for the Er-167 isotope in $ScPO_4$, YPO_4, and $LuPO_4$ are 1.00, 1.01, and 1.00, respectively, which indicates that admixtures from other higher lying J states may be neglected.

E. Trivalent ytterbium

Yb^{3+} has a $4f^{13}$ electronic configuration and a $^2F_{7/2}$ free-ion ground state. The eightfold ground state degeneracy is split by the tetragonal crystal field into four Kramers' doublets and the EPR spectrum observed at $T = 4.2$ K arises from transitions within the ground doublet. Yb^{3+} EPR spectra with tetragonal symmetry were detected in all three orthophosphate hosts. Figure 6 shows the spectra obtained using a $LuPO_4$ crystal doped with enriched Yb-171. The measured experimental principal g values and hyperfine parameters are listed in Tables I and II, respectively.

The wave functions describing the magnetic properties of the Yb^{3+} ground doublet in tetragonal symmetry sites will have one of the following two forms:

$$a|\pm 7/2\rangle + b|\mp 1/2\rangle ,$$

or

$$c|\pm 5/2\rangle + d|\mp 3/2\rangle .$$

The g principal values corresponding to these states are either:

$$g_\parallel = \lambda(7a^2 - b^2) \text{ and } g_\perp = 4\lambda b^2$$

or

$$g_\parallel = \lambda(5c^2 - 3d^2) \text{ and } g_\perp = \sqrt{48}\,\lambda cd ,$$

where the first order value of λ, the Landé factor, is equal to 8/7. For the present results, the measured g values are found to fit the second form more closely. The same wave function has been used to describe the Yb^{3+} ground doublet in a series of scheelite type hosts,[28,55] where the rare-earth ion is in tetragonal symmetry sites as well as tetragonal symmetry Yb^{3+} spectra observed in cubic CaF_2,[38,56] cubic AgCl,[57] and the zircon-types YPO_4[30] and $ThSiO_4$.[54] On the other hand, a wave function of the first form must be used for the tetragonal Yb^{3+} spectra observed in cubic CaO,[58] cubic KM_gF_3,[42] and the zircon structure hosts YVO_4[29] and $HfSiO_4$.[54] The experimental g values obtained for Yb^{3+} in another zircon type host $YAsO_4$,[51] can be accounted

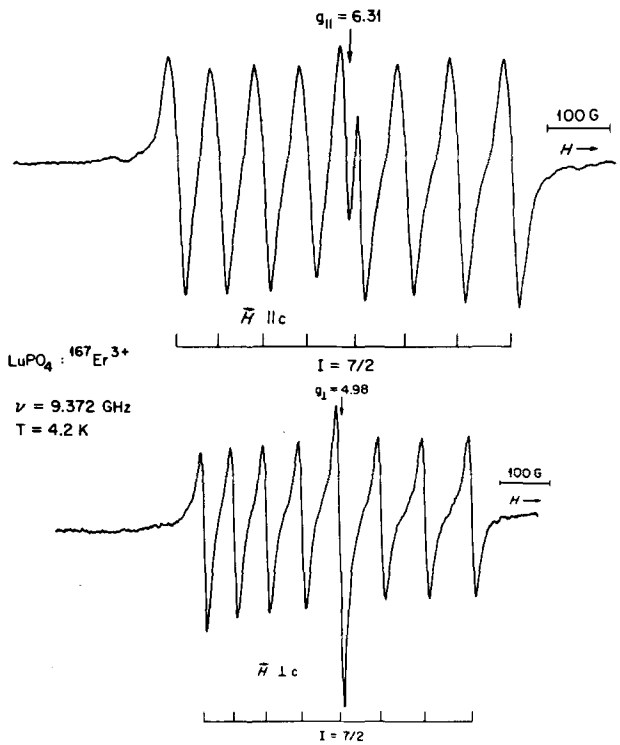

FIG. 5. EPR spectra of a $LuPO_4$ crystal doped with isotopically enriched erbium-167. Top trace—spectrum with H parallel to the c axis; bottom trace—spectrum with H perpendicular to the c axis. The hyperfine lines are identified by the bar diagram below the traces. A central line due to some residual even erbium isotopes is present and is superimposed on an erbium-167 hyperfine line in the bottom trace. The relative intensities are due to the artificial enrichment.

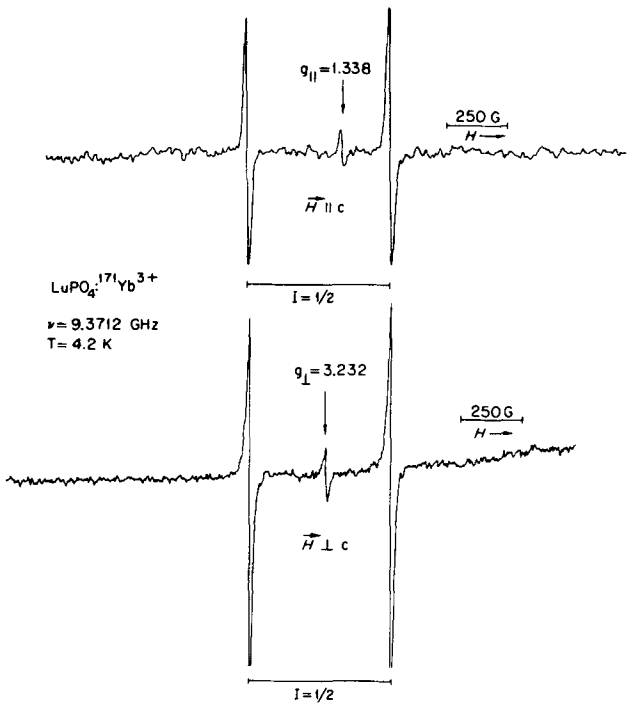

FIG. 6. EPR spectra of a $LuPO_4$ crystal doped with isotopically enriched ytterbium-171. Top trace—spectrum with H parallel to the c axis; bottom trace—spectrum with H perpendicular to the c axis. The small central line in each trace is due to the even–even isotopes of ytterbium with zero nuclear spin. The absence of the normally occurring ytterbium-173 isotope is a result of the artificial enrichment. The second-order shift to lower magnetic fields for the ytterbium-171 hyperfine lines is greater in the parallel orientation (top trace) than in the perpendicular orientation.

for by either of the two possible wave functions. A curve showing the range of possible g values for each of the two wave function forms has been given by Sattler and Nemarich.[55] The experimental g and A values for the Yb-171 isotope yield values of 0.98, 0.99, and 0.98 for the Elliott and Stevens' parameter,[25] $g_{\parallel}B/g_{\perp}A$, in $ScPO_4$, YPO_4, and $LuPO_4$, respectively. The corresponding values of 1.04, 1.04, and 1.03 are obtained for the Yb-173 isotope. Again, this indicates that admixtures from higher lying J states are probably negligible.

F. Trivalent uranium

U^{3+} has a $5f^3$ electronic configuration and a $^4I_{9/2}$ ground state and therefore its behavior in a crystal field will be similar to that of its rare-earth analog Nd^{3+} which has a $4f^3$ electronic configuration. As a consequence, the observation of the Nd^{3+} spectrum in a particular host facilitates the identification of a U^{3+} spectrum in the same host. This can be particularly important in many cases due to the absence of hyperfine structure for the 99.3% naturally abundant isotope U-238. At T=4.2 K, a single EPR line was observed in both the uranium-doped $ScPO_4$ and uranium-doped $LuPO_4$ crystals. This spectrum was attributed to trivalent uranium in substitutional sites of tetragonal symmetry. A graph of the square of the g value in $LuPO_4$ vs $\cos^2\Theta$ is shown in Fig. 7 where Θ is the angle between the applied magnetic field and the tetragonal c axis. The U^{3+} line width, which was ~10 G at $\Theta=0°$, became progressively wider as the perpendicular direction was approached. Near $\Theta=90°$, the resonance line became so broad that it was almost unobservable. Therefore, the value of $g_{\perp}$ had to be obtained by a least-squares fit to the data shown in Fig. 7. On the other hand, for the case of $ScPO_4$: U^{3+}, the linewidth was wider at $\Theta=0°$ (~20 G) than at $\Theta=90°$ (~10 G). The experimental g values for U^{3+} in $ScPO_4$ and $LuPO_4$ are tabulated in Table I. The U^{3+} spectrum was not observed in YPO_4.

The EPR spectrum of U^{3+} in tetragonal symmetry sites has been reported only in the case of the alkaline earth fluorides CaF_2,[26,59–62] SrF_2,[26,63] and BaF_2[64] with average $\bar{g}$ values ranging between 2.0 and 2.5. Bleaney *et al.*[26] compared the U^{3+} spectra with the Nd^{3+} spectra in these hosts and concluded that a wave function of the form $\alpha|\pm 9/2\rangle + \beta|\pm 1/2\rangle + \gamma|\mp 7/2\rangle$ was most likely for both ions.

Optical absorption studies of single crystals of monoclinic $LaPO_4$ have previously shown that uranium is incorporated in this material in a predominantly tetravalent state and that only about 5% of the uranium ions were in the form of U^{3+}.[11] The EPR spectrum of tetravalent uranium has been investigated previously in the fluorite-structure alkaline earth halides CaF_2, SrF_2,

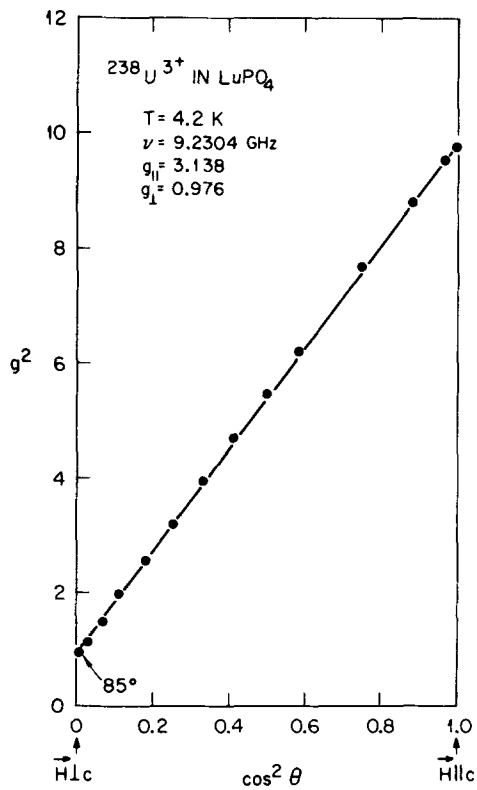

FIG. 7. Plot of square of the effective g value vs $\cos^2\theta$ obtained from EPR data for trivalent uranium in a single crystal of $LuPO_4$. Theta is the angle between the applied magnetic field and the crystal c axis. The resonance line was almost unobservable at $\theta=90°$ and, therefore, this plot was used to determine the value of $g_{\perp}$.

and BaF_2[85] and, in each case, the U^{4+} ions occupied trigonal sites with $g_{\parallel}$ values ranging from 5.66 to 2.87 and $g_{\perp}$ values close to zero. In fact, the theoretical maximum of $g_{\parallel}$ for the non-Kramers' U^{4+} ion should be 8λ or 6.4 and $g_{\perp}$ should be identically zero. In the present case of the tetragonal symmetry hosts $ScPO_4$, YPO_4, and $LuPO_4$ doped with uranium, no EPR spectra were observed that could be identified with the presence of tetravalent uranium.

IV. SUMMARY AND CONCLUSIONS

Investigations of the EPR spectra of five different trivalent rare-earth ions and one trivalent actinide ion incorporated as dilute impurities in the tetragonal symmetry hosts $ScPO_4$, YPO_4, and $LuPO_4$ have been carried out. Determinations of the principal g values and hyperfine parameters were made and these results have been used in deriving information regarding the nature of the ground doublets in those cases in which such a determination could be made. The lanthanide orthophosphates represent a promising new class of nuclear and transuranic waste forms and information concerning the solid state chemistry of actinide dopants in these materials is germane to their application in this technologically important role. Additionally, since complex wastes such as reprocessed spent nuclear reactor fuels may contain up to 35 wt. % rare-earth oxides, the behavior of mixed rare-earth systems is of considerable practical importance. In the present work it has been shown that a wide variety of these waste oxides can be incorporated in mixed orthophosphates, and that the application of EPR techniques in determining the valence states of various impurities and obtaining information regarding the location of ions in the host orthophosphate lattice can represent an important capability in the evaluation of these materials as radioactive waste forms

ACKNOWLEDGMENT

The authors are indebted to Lazelle S. Tyler for her help in preparing the manuscript.

[1]G. W. Beall, L. A. Boatner, D. F. Mullica, and W. O. Milligan, J. Inorg. Nucl. Chem. **43**, 101 (1981).
[2]L. A. Boatner, G. W. Beall, M. M. Abraham, C. B. Finch, P. G. Huray, and M. Rappaz, *Scientific Basis for Nuclear Waste Management*, edited by C. J. Northrup (Plenum, New York, 1980), Vol. II, p. 289.
[3]M. M. Abraham, L. A. Boatner, G. W. Beall, C. B. Finch, R. J. Floran, P. G. Huray, and M. Rappaz, in *Alternate Nuclear Waste Forms and Interactions in Geologic Media*, CONF-8005107, edited by L. A. Boatner and C. C. Battle, Jr. (U. S. DOE, Washington, D.C., 1981), p. 144.
[4]L. A. Boatner, G. W. Beall, M. M. Abraham, C. B. Finch, R. J. Floran, P. G. Huray, and M. Rappaz, *Management of Alpha-Contaminated Wastes*, IAEA-SM 246/73 (IAEA, Vienna, 1981), p. 411.
[5]M. M. Abraham, L. A. Boatner, and M. Rappaz, Phys. Rev. Lett. **45**, 839 (1980).
[6]M. Rappaz, M. M. Abraham, J. O. Ramey, and L. A. Boatner, Phys. Rev. B **23**, 1012 (1981).
[7]M. Rappaz, L. A. Boatner, and M. M. Abraham, J. Chem. Phys. **73**, 1095 (1980).
[8]M. Rappaz, J. O. Ramey, L. A. Boatner, and M. M. Abraham, J. Chem. Phys. **76**, 40 (1982).
[9]T. Hayhurst, G. Shalimoff, N. Edelstein, L. A. Boatner, and M. M. Abraham, J. Chem. Phys. **74**, 5449 (1981).
[10]T. Hayhurst, G. Shalimoff, J. G. Conway, N. Edelstein, L. A. Boatner, and M. M. Abraham, J. Chem. Phys. **76**, 3960 (1982).
[11]K. L. Kelley, G. W. Beall, J. P. Young, and L. A. Boatner, *Scientific Basis for Nuclear Waste Management*, edited by J. G. Moore (Plenum, New York, 1981), Vol. 3, p. 189.
[12]W. O. Milligan, D. F. Mullica, G. W. Beall, and L. A. Boatner, Inorg. Chim. Acta **60**, 39 (1982).
[13]G. M. Begun, G. W. Beall, L. A. Boatner, and W. T. Gregor, J. Raman Spectrosc. **11**, 273 (1981).
[14]R. S. Feigelson, J. Am. Ceram. Soc. **47**, 257 (1964).
[15]See, for example, R. W. Reynolds, Y. Chen, L. A. Boatner, and M. M. Abraham, Phys. Rev. Lett. **29**, 18 (1972).
[16]J. M. Baker, W. Hayes, and D. A. Jones, Proc. Phys. Soc. London **73**, 942 (1959).
[17]M. Dvir and W. Low, Proc. Phys. Soc. London **75**, 136 (1960).
[18]A. A. Antipin, I. N. Kurkin, G. K. Chirkin, and L. Ya. Shekun, Fiz. Tverd. Tela **6**, 2014 (1964) [Sov. Phys. Solid State **6**, 1590 (1965)].
[19]S. D. McLaughlan, Phys. Rev. **160**, 287 (1967).
[20]A. Kafri, D. Kiro, S. Yatsiv, and W. Low, Solid State Commun. **6**, 573 (1968). There is a misprint for the traces quoted in this reference.
[21]I. N. Kurkin, A. M. Morozov, and L. Ya. Shekun, DAN SSSR **161**, 322 (1965) [Sov. Phys. Dokl. **10**, 225 (1965)].
[22]I. N. Kurkin and L. Ya. Shekun, Fiz. Tverd. Tela **7**, 2852 (1965) [Sov. Phys. Solid State **7**, 2308 (1965)].
[23]A. A. Antipin, I. N. Kurkin, L. I. Potkin, and L. Ya. Shekun, Fiz. Tverd. Tela **8**, 2808 (1966) [Sov. Phys. Solid State **8**, 2247 (1967)].
[24]R. S. Rubins, Phys. Rev. B **1**, 139 (1970).
[25]R. J. Elliott and K. W. H. Stevens, Proc. R. Soc. London Ser. A **218**, 553 (1953).
[26]B. Bleaney, P. M. Llewellyn, and D. A. Jones, Proc. Phys. Soc. London Sect. B **69**, 858 (1956).
[27]See I. N. Kurkin, Fiz. Tverd. Tela **8**, 731 (1966) [Sov. Phys. Solid State **8**, 585 (1966)], and references therein.
[28]J. P. Sattler and J. Nemarich, Phys. Rev. B **4**, 1 (1971).
[29]U. Ranon, Phys. Lett. A **28**, 228 (1968).
[30]W. Hillmer, Phys. Status Solidi B **47**, 133 (1971).
[31]A. A. Antipin, I. N. Kurkin, L. Z. Potvorova, and L. Ya. Shekun, Fiz. Tverd. Tela **7**, 3685 (1965) [Sov. Phys. Solid State **7**, 2979 (1966)].
[32]D. Ball, Phys. Status Solidi B **46**, 635 (1971).
[33]U. Ranon, J. C. Danner, and D. N. Stamires, Bull. Am. Phys. Soc. **13**, 1671 (1968).
[34]W. Hillmer, J. Plamper, and D. Wappler, Phys. Status Solidi B **50**, 507 (1972).
[35]M. J. Weber and R. W. Bierig, Phys. Rev. A **134**, 1492 (1964).
[36]U. Ranon and W. Low, Phys. Rev. **132**, 1609 (1963).
[37]Yu. K. Voron'ko, G. M. Zverev, B. B. Meshkov, and A. I. Smirnov, Fiz. Tverd. Tela **6**, 2799 (1965) [Sov. Phys. Solid State **6**, 2225 (1965)].
[38]L. S. Kornienko and A. O. Rybaltovskii, Fiz. Tverd. Tela **15**, 1975 (1973) [Sov. Phys. Solid State **15**, 1322 (1974)].
[39]M. R. Brown, K. G. Roots, J. M. Williams, W. A. Shand, C. Groter, and H. F. Kay, J. Chem. Phys. **50**, 891 (1969).
[40]G. M. Zverev and A. I. Smirnov, Fiz. Tverd. Tela **6**, 96 (1964) [Sov. Phys. Solid State **6**, 76 (1964)].
[41]I. C. Chang and W. W. Anderson, Phys. Lett. **13**, 112 (1964).
[42]M. M. Abraham, C. B. Finch, J. L. Kolopus, and J. T. Lewis, Phys. Rev. B **3**, 2855 (1971).
[43]D. R. Mason and C. Kikuchi, Phys. Lett. A **28**, 260 (1968).
[44]J. Kirton, Phys. Rev. A **139**, 1930 (1965).
[45]Yu. A. Bobrovnikov, G. M. Zverev, and A. I. Smirnov, Fiz. Tverd. Tela **9**, 1794 (1967) [Sov. Phys. Solid State **9**, 1403 (1967)].

[46]I. V. Vasil'ev, G. M. Zverev, L. V. Makarenko, L. I. Plotkin, and A. I. Smirnov, Fiz. Tverd. Tela **11**, 776 (1969) [Sov. Phys. Solid State **11**, 625 (1969)].
[47]I. N. Kurkin and E. A. Tsvetkov, Fiz. Tverd. Tela **11**, 3610 (1969) [Sov. Phys. Solid State **11**, 3027 (1970)].
[48]M. R. Brown, K. G. Roots, and W. A. Shand, J. Phys. C **2**, 593 (1969).
[49]A. A. Antipin, A. N. Katyshev, I. N. Kurkin, and L. Ya. Shekun, Fiz. Tverd. Tela **10**, 595 (1968) [Sov. Phys. Solid State **10**, 468 (1968)].
[50]G. M. Zverev, L. V. Makarenko, and A. I. Smirnov, Fiz. Tverd. Tela **9**, 3651 (1968) [Sov. Phys. Solid State **9**, 2883 (1968)].
[51]J. Plamper, Phys. Status Solidi B **47**, 129 (1971).
[52]M. Dzionara, H. A. Kahle, and F. Schwedewie, Phys. Status Solidi B **47**, 135 (1971).
[53]W. Hintzman, Z. Phys. **230**, 213 (1970).
[54]R. W. Reynolds, L. A. Boatner, C. B. Finch, A. Châtelain, and M. M. Abraham, J. Chem. Phys. **56**, 5607 (1972).
[55]See J. P. Sattler and J. Nemarich, Phys. Rev. B **1**, 4249 (1970), and references therein.
[56]See J. Kirton and S. D. McLaughlan, Phys. Rev. **155**, 279 (1967), and references therein.
[57]F. B. I. Cook and M. J. A. Smith, J. Phys. C **6**, 3785 (1973).
[58]R. W. Reynolds, L. A. Boatner, Y. Chen, and M. M. Abraham, J. Chem. Phys. **60**, 1593 (1974).
[59]A. Yariv, Phys. Rev. **128**, 1588 (1962).
[60]M. M. Abraham (unpublished), reported by L. A. Boatner and M. M. Abraham, Rep. Prog. Phys. **41**, 87 (1978).
[61]T. D. Black and P. L. Donoho, Phys. Rev. **170**, 462 (1968).
[62]V. Lupei, C. Stoicescu, and I. Ursu, J. Phys. C **9**, L317 (1976).
[63]E. D. Dahlberg and T. D. Black, Phys. Rev. B **10**, 3756 (1974).
[64]B. G. Berulava and G. I. Sanadze, *Paramagnetic Resonance* (Kazan, USSR, 1960), p. 11.
[65]See L. A. Boatner and M. M. Abraham, Rep. Prog. Phys. **41**, 87 (1978), and references therein.